

Violation of Wiedemann-Franz Law for a Hot Hadronic Matter created at NICA, FAIR and RHIC Energies using Non-extensive Statistics

Rutuparna Rath, Sushanta Tripathy, Bhaswar Chatterjee, and Raghunath Sahoo*
Discipline of Physics, School of Basic Sciences, Indian Institute of Technology Indore, Simrol, Indore- 453552, INDIA

Swatantra Kumar Tiwari
Department of Applied Science and Humanities, Muzaffarpur Institute of Technology, Muzaffarpur- 842003, Bihar

Abhishek Nath
Department of Physical Sciences, Indian Institute of Science Education and Research, Kolkata-741246, India
 (Dated: October 20, 2022)

We present here the computation of electrical and thermal conductivity by solving the Boltzmann transport equation in relaxation time approximation. We use the q -generalized Boltzmann distribution function to incorporate the effects of non-extensivity. The behaviour of these quantities with changing temperature and baryochemical potential has been studied as the system slowly moves towards thermodynamic equilibrium. We have estimated the Lorenz number at NICA, FAIR and the top RHIC energies and studied as a function of temperature, baryochemical potential and the non-extensive parameter, q . We have observed that Wiedemann-Franz law is violated for a non-extensive hadronic phase.

PACS numbers: 12.38.Mh, 24.10.Pa, 24.10.Nz, 25.75.-q, 47.75.+f

I. INTRODUCTION

The ultra-relativistic heavy-ion collision experiments like RHIC at BNL and LHC at CERN provide a brief opportunity to look into a strongly interacting hot and dense matter consisting of deconfined quarks and gluons at an extreme temperature and/or energy density. The thermalized system of deconfined quarks and gluons, known as quark-gluon plasma (QGP) undergoes a phase transition to a system with hadronic degrees of freedom, which is known as the hadron gas (HG) phase as the system cools down. Large elliptic flow observed at Relativistic Heavy Ion Collider (RHIC) hints that QGP is a strongly coupled near perfect fluid which necessitates a small but finite shear viscosity to entropy density ratio ($\frac{\eta}{s}$). The lowest bound of shear viscosity to entropy ratio (η/s) is $1/4\pi$ as conjectured by AdS/CFT correspondence known as Kovtun-Son-Starinets (KSS) bound [1]. The measurements of elliptic flow in experiments like RHIC and LHC suggest that the system formed by the heavy-ion collisions have η/s close to KSS bound [2, 3]. This signifies the importance of studying the transport properties to understand the hydrodynamic evolution properly.

In addition to the coefficients of viscosity, elliptic flow can also be significantly affected if there is some external or internal source of anisotropy. It has been suggested that extremely strong magnetic field ($\sim m_\pi^2$) might get produced at high energy collisions depending on centrality. Initially the magnetic field was thought to decay rapidly after collision [4]. However, it has been pointed

out that the electric field induced by a rapidly decaying magnetic field would resist farther decay and satisfy diffusion equation [5]. One crucially important thing in such a scenario is the electrical conductivity (σ_{el}) of the medium. Additionally, σ_{el} also plays an important role in low mass dilepton production and the hydrodynamic evolution. So a proper estimation of σ_{el} would be beneficial for overall better understanding of heavy ion collision events. Various methods have been proposed to estimate σ_{el} like chiral perturbation theory [6], the numerical simulation of Boltzmann equation [7], holography [8], transport models [9], Dyson-Schwinger equation [10] etc. Most of these calculations are for QGP and to understand the phase transition from QGP to HG, it is very important to learn about the electrical conductivity in HG.

Another critically important but less explored aspect of heavy ion collision is heat conduction. At very high energy collision events, this may be of lesser importance as the net baryon density is very small. But at NICA and FAIR energies as well as at low energy runs at RHIC, baryon density can be significant and heat conduction can play a major role in the evolution of the system. In the hadronic phase, thermal conductivity (κ) has been calculated for pion gas by assigning a pion chemical potential as pion numbers can be taken to be constant in the late stage of the evolution [11]. Recently it has also been calculated for baryonic matter within hadron resonance gas (HRG) model [12].

To describe the particle production mechanism and study the QCD thermodynamics, the statistical models are more useful due to high multiplicities produced in high-energy collisions. It has been proposed that the transverse momentum (p_T) spectra of final state particles produced in high-energy collisions would follow a thermalized Boltzmann-Gibbs (BG) distribution. However,

*Electronic address: Raghunath.Sahoo@cern.ch

a finite degree of deviation from the BG distribution of the p_T -spectra has been observed by the RHIC [13, 14] and LHC [15–17] experiments. Also, the matter produced in these extreme conditions evolves rapidly in non-homogenous way. Thus, the global equilibrium is not necessarily established and some of the observables become non-extensive. Also, a power-law tail develops in the p_T -spectra instead of exponential distributions. Similar behavior could also be due to local temperature fluctuation and long-range correlations in the produced system [18]. In such cases instead of using BG statistics, a generalized non-extensive statistics [19, 20] might give us more insight. Recently, growing attention has been paid towards explaining the particle spectra in high-energy hadronic and heavy-ion collisions [21–26]. Using Tsallis non-extensive statistics in Boltzmann transport equation (BTE) with relaxation time approximation (RTA) has successfully explained the elliptic flow [27] and nuclear modification factor [28, 29] of identified particles. The dissipative properties such as shear and bulk viscosity has been reported using the non-extensive Boltzmann Transport Equation (NBTE) in RTA [30].

In this work, we study the behaviour of σ_{el} and κ with temperature at finite baryon chemical potential, μ_B in non-extensive scenario. We use the non-extensive Boltzmann distribution function and solve the BTE using RTA to obtain σ_{el} and κ and study their behaviour for different values of the non-extensive parameter. We also calculate the ratio of the two coefficients to examine the validity of Wiedemann-Franz law which was originally proposed for free electron metals.

We have organized the paper in the following manner. In the Sect. II, we derive electrical and thermal conductivities for hadronic degrees of freedom using BTE in RTA. Here, we take q -equilibrium as a solution of BTE. Section III presents the discussion of results obtained using the formulation. In Sect. IV, the summary and conclusions of this work are presented.

II. FORMULATION

A. Electrical Conductivity

The transport properties such as electrical conductivity and thermal conductivity for a hadronic matter using non-extensive statistics has been calculated by the technique mentioned in Ref. [31, 32]. From the Relativistic Boltzmann Transport equation, we can initiate our derivation of transport coefficients which is given by,

$$p^\mu \partial_\mu f_p(x, p) + Q_a F^{\alpha\beta} p_\beta \frac{\partial f_a(x, p)}{\partial p^\alpha} = C_a[f_a], \quad (1)$$

where p^μ is the momentum four vector, Q_a is the electric charge of the a^{th} particle, $f_a(x, p)$ is the particle distribution function when system is away from equilibrium, index a is used in the distribution function for differ-

ent hadronic species and $F^{\alpha\beta}$ is the electromagnetic field strength tensor, which is given by,

$$\begin{pmatrix} 0 & -E_x & -E_y & -E_z \\ E_x & 0 & 0 & 0 \\ E_y & 0 & 0 & 0 \\ E_z & 0 & 0 & 0 \end{pmatrix}$$

$C_a[f_a]$ is the collision integral term which is approximated using the relaxation-time approximation (RTA) and given by

$$C_a[f_a] \simeq -\frac{p^\mu u_\mu}{\tau_a} \delta f_a, \quad (2)$$

where $u_\mu = (1, \mathbf{0})$ is the fluid four velocity in the local rest frame and τ_a is the relaxation time of the system, which is the time required by the system to reach the q -equilibrium.

Considering the system being relaxed towards the equilibrium state, we can take the function in the form:

$$f_a(x, p) = f_a^0(x, p) + \delta f_a = f_a^0(x, p)[1 + \phi(x, p)], \quad (3)$$

where $\phi(|\phi| \ll 1)$ is used for perturbation. We have taken the non-extensive Tsallis distribution as f_a^0 [33] near the local rest frame of the fluid, where the system is described locally by temperature, T , baryochemical potential, μ_B and fluid velocity, u_μ , which change slowly in space and time [34]. In Boltzmann's approximation, the thermodynamically consistent Tsallis distribution is given as,

$$f_a^0 = \frac{1}{\left[1 + (q-1)\left(\frac{p^\mu u_\mu - \mu}{T}\right)\right]^{\frac{q}{q-1}}}, \quad (4)$$

where \mathbf{u} is the fluid velocity. q is the non-extensive parameter, which signifies how far the system is away from thermodynamic equilibrium. T and $\mu = B\mu_B + s\mu_s$ are temperature and chemical potential, respectively. Here we consider only the baryochemical potential, μ_B , ignoring the strangeness chemical potential. By applying local equilibrium approximation ($f_a \equiv f_a^0$) in the LHS of BTE, we obtain:

$$Q_a \left(p_0 \mathbf{E} \cdot \frac{\partial f_a^0}{\partial \mathbf{p}} + \mathbf{E} \cdot \mathbf{p} \frac{\partial f_a^0}{\partial p_0} \right) = -\frac{p_0}{\tau_a} \delta f_a. \quad (5)$$

Now, for a constant electric field \mathbf{E} , Eq. (5) becomes

$$\delta f_a = q \frac{Q_a \tau_a \mathbf{E} \cdot \mathbf{p}}{T p_0} f_0^{(2q-1)/q}. \quad (6)$$

As we know, the electrical conductivity is a parameter which quantifies the response of the system to an applied electric field. Using the relationship between electric current (\mathbf{j}) and applied electric field (\mathbf{E}), one can have the

expression for σ_{el} as,

$$\mathbf{j} = \sigma_{el} \mathbf{E}. \quad (7)$$

The four current, $j^\mu = (j, \mathbf{j})$ is defined as,

$$j^\mu = Q_a g_a \int \frac{d^3 p}{(2\pi)^3 E_a} p^\mu f_a(x, p), \quad (8)$$

where g_a is the degeneracy and $E_a^2 = p^2 + m_a^2$ is the energy dispersion relation for the a^{th} hadron species. When we are slightly away from the equilibrium, we can apply the approximation mentioned in Eq. (3) to j^μ and obtain the four current as:

$$j^\mu = j_0^\mu + \Delta j^\mu. \quad (9)$$

So,

$$\begin{aligned} j^\mu &= Q_a g_a \int \frac{d^3 p}{(2\pi)^3 E_a} p^\mu f_a + Q_a g_a \int \frac{d^3 p}{(2\pi)^3 E_a} p^\mu \delta f_a \\ &= j_0^\mu + \Delta j^\mu, \end{aligned} \quad (10)$$

and

$$\Delta j^\mu = Q_a g_a \int \frac{d^3 p}{(2\pi)^3 E_a} p^\mu \delta f_a, \quad (11)$$

Using local equilibrium approximation, we can write

$$\mathbf{j} = \Delta \mathbf{j} = \sigma_{el} \mathbf{E}. \quad (12)$$

Using Eq. 6, 11 and 12 the electrical conductivity (σ_{el}) can be evaluated. We can start with E_x component:

$$\begin{aligned} \Delta j^x &= Q_a^2 g_a \int \frac{d^3 p \tau_a}{T (2\pi)^3 E_a^2} p_x (E_x p_x + E_y p_y \\ &\quad + E_z p_z) q f_0^{(2q-1)/q} \\ &= \sigma_{xx} E_x + \sigma_{xy} E_y + \sigma_{xz} E_z. \end{aligned} \quad (13)$$

Since electrical conductivity is related to the E_x part of the above equation, we can define (using the fact that $p_x = p_y = p_z = \frac{p}{3}$)

$$\sigma_{xx} E_x = \sigma_{el} E_x = Q_a^2 g_a \int \frac{d^3 p p^2 \tau_a}{3T (2\pi)^3 E_a^2} q f_0^{(2q-1)/q} E_x. \quad (14)$$

Hence,

$$\sigma_{el} = \frac{1}{3T} \sum_a Q_a^2 g_a \int \frac{d^3 p p^2 \tau_a}{(2\pi)^3 E_a^2} q f_0^{(2q-1)/q}. \quad (15)$$

B. Thermal Conductivity

The heat flow in the interacting systems can be described by the quantity called thermal conductivity κ . The energy momentum tensor $T^{\mu\nu}$ and the four current j^μ is given by;

$$T^{\mu\nu} = g_a \int \frac{d^3 p p^\mu p^\nu}{(2\pi)^3 E_a} f_a(x, p), \quad (16)$$

$$j^\mu = g_a \int \frac{d^3 p p^\mu}{(2\pi)^3 E_a} f_a(x, p). \quad (17)$$

For a small perturbation from the equilibrium, the change in the energy momentum tensor $\Delta T^{\mu\nu}$ and the four current Δj^μ can be written as,

$$\Delta T^{\mu\nu} = g_a \int \frac{d^3 p p^\mu p^\nu}{(2\pi)^3 E_a} \delta f_a, \quad (18)$$

$$\Delta j^\mu = g_a \int \frac{d^3 p p^\mu}{(2\pi)^3 E_a} \delta f_a. \quad (19)$$

The δf_a term can be evaluated from the collision term present in the above BTE in the absence of external field. Hence one can write,

$$p^\mu \partial_\mu f_a(x, p) = -\frac{p^\mu u_\mu}{\tau_a} \delta f_a, \quad (20)$$

where $\partial_\mu = u_\mu D + \nabla_\mu$ and the convective derivatives (DT, D_μ, Du^μ) can be decimated by using the following relations as done in [32];

$$(\epsilon + P) Du^\mu - \nabla^\mu P = 0, \quad (21)$$

$$Dn + n \nabla_\mu u^\mu = 0. \quad (22)$$

Using the above two relations, $\Delta T^{\mu\nu}$ and Δj^μ can be written as,

$$\begin{aligned} \Delta T^{\mu\nu} &= g_a \int \frac{d^3 p}{(2\pi)^3 E_a} \frac{p^\mu p^\nu}{p \cdot u} \frac{1}{T} \left[\tau_a q f_0^{(2q-1)/q} \left\{ p \cdot u \left(\frac{\partial p}{\partial \epsilon} \right)_n \right. \right. \\ &\quad \nabla_\alpha u^\alpha + p^\alpha X_\alpha + \frac{p^\alpha p^\beta}{p \cdot u} \nabla_\alpha u_\beta + \left(\frac{\partial p}{\partial n} \right)_\epsilon \nabla_\alpha u^\alpha \\ &\quad \left. \left. - \frac{\epsilon + P}{n} \frac{p^\alpha}{p \cdot u} X_\alpha \right\} \right], \end{aligned} \quad (23)$$

$$\begin{aligned} \Delta j^\mu = g_a \int \frac{d^3 p}{(2\pi)^3 E_a} \frac{p^\mu}{p \cdot u} \frac{1}{T} \left[\tau_a q f_0^{(2q-1)/q} \left\{ p \cdot u \left(\frac{\partial p}{\partial \varepsilon} \right)_n \right. \right. \\ \left. \left. \nabla_\alpha u^\alpha + p^\alpha X_\alpha + \frac{p^\alpha p^\beta}{p \cdot u} \nabla_\alpha u_\beta + \left(\frac{\partial p}{\partial n} \right)_\varepsilon \nabla_\alpha u^\alpha \right. \right. \\ \left. \left. - \frac{\varepsilon + P}{n} \frac{p^\alpha}{p \cdot u} X_\alpha \right\} \right], \end{aligned} \quad (24)$$

where

$$X_\alpha = \frac{\nabla_\alpha P}{\varepsilon + P} - \frac{\nabla_\alpha T}{T}, \quad (25)$$

and $u_\mu = (1, \mathbf{0})$. ε and n are the energy density and number density respectively. $T^{0i} = \Delta T^{0i} - \frac{(\varepsilon + P)}{n} \Delta j^i \equiv I^i$.

$$\Delta T^{0i} = \sum_a g_a \int \frac{d^3 p}{(2\pi)^3} \frac{\mathbf{p}^2}{3T} \tau_a q f_0^{(2q-1)/q} \left\{ 1 - \frac{\varepsilon + P}{n E_a} \right\} X_i \quad (26)$$

and

$$\Delta j^i = \sum_a g_a \int \frac{d^3 p}{(2\pi)^3 E_a} \frac{\mathbf{p}^2}{3T} \tau_a q f_0^{(2q-1)/q} \left\{ 1 - \frac{\varepsilon + P}{n E_a} \right\} X_i. \quad (27)$$

Using the Eckart or Landau-Lifshitz condition, heat conductivity can be defined as,

$$I^i = -\kappa [\partial_i T - T \partial_i P / (\varepsilon + P)] = \kappa T X_i. \quad (28)$$

Now the thermal conductivity is defined as,

$$\kappa = \frac{1}{3T^2} \sum_a g_a \tau_a \int \frac{d^3 p}{(2\pi)^3} \frac{\mathbf{p}^2}{E_a^2} q f_0^{(2q-1)/q} \left(E_a - \frac{t_a \omega}{n} \right)^2, \quad (29)$$

where $\omega = \varepsilon + P$ is the enthalpy and $t_a = +1(-1)$ for particles (anti-particles).

C. Relaxation Time

The energy dependent relaxation time is stated as,

$$\tau^{-1}(E_a) = \sum_{bcd} \int \frac{d^3 p_b d^3 p_c d^3 p_d}{(2\pi)^3 (2\pi)^3 (2\pi)^3} W(a, b \rightarrow c, d) f_b^0, \quad (30)$$

where the transition rate $W(a, b \rightarrow c, d)$ is defined as,

$$W(a, b \rightarrow c, d) = \frac{2\pi^4 \delta(p_a + p_b - p_c - p_d)}{2E_a 2E_b 2E_c 2E_d} |\mathcal{M}|^2, \quad (31)$$

and the transition amplitude is $|\mathcal{M}|$. By considering the center-of-mass frame, Eq. 30 can be simplified as,

$$\begin{aligned} \tau^{-1}(E_a) &= \sum_b \int \frac{d^3 p_b}{(2\pi)^3} \sigma_{ab} \frac{\sqrt{s - 4m^2}}{2E_a 2E_b} f_b^0 \\ &\equiv \sum_b \int \frac{d^3 p_b}{(2\pi)^3} \sigma_{ab} v_{ab} f_b^0, \end{aligned} \quad (32)$$

where, v_{ab} and \sqrt{s} are the relative velocity and the center-of-mass energy, respectively. The total scattering cross-section in the process $a(p_a) + b(p_b) \rightarrow a(p_c) + b(p_d)$ is given by σ_{ab} . $\tau(E_a)$ can be approximated to averaged relaxation time ($\tilde{\tau}$) [35] for further simplification and it can be done by averaging over f_a^0 using Eq. 32 and given as,

$$\begin{aligned} \tilde{\tau}_a^{-1} &= \frac{\int \frac{d^3 p_a}{(2\pi)^3} \tau^{-1}(E_a) f_a^0}{\int \frac{d^3 p_a}{(2\pi)^3} f_a^0} \\ &= \sum_b \frac{\int \frac{d^3 p_a}{(2\pi)^3} \frac{d^3 p_b}{(2\pi)^3} \sigma_{ab} v_{ab} f_a^0 f_b^0}{\int \frac{d^3 p_a}{(2\pi)^3} f_a^0} \\ &= \sum_b n_b \langle \sigma_{ab} v_{ab} \rangle, \end{aligned} \quad (33)$$

here n_b is the number density of b^{th} hadronic species. The thermal average for the scattering of same species of particles at a given T and μ_B with constant cross-section can be calculated as, follows [31, 36, 37].

$$\langle \sigma_{ab} v_{ab} \rangle = \frac{\sigma \int d^3 p_a d^3 p_b v_{ab} e_q^{-(E_a - \mu_B)/T} e_q^{-(E_b - \mu_B)/T}}{\int d^3 p_a d^3 p_b e_q^{-(E_a - \mu_B)/T} e_q^{-(E_b - \mu_B)/T}}. \quad (34)$$

The momentum space volume elements can be written as,

$$d^3 p_a d^3 p_b = 8\pi^2 p_a p_b dE_a dE_b d\cos\theta. \quad (35)$$

The numerator in Eq. 34 is written as,

$$\sigma \int d^3 p_a d^3 p_b v_{ab} e_q^{-E_a/T} e_q^{-E_b/T} = \sigma \int 8\pi^2 p_a p_b dE_a dE_b d\cos\theta e_q^{-E_a/T} e_q^{-E_b/T} \times \frac{\sqrt{(E_a E_b - p_a p_b \cos\theta)^2 - (m_a m_b)^2}}{E_a E_b - p_a p_b \cos\theta} \quad (36)$$

and the denominator is written as,

$$\int d^3p_a d^3p_b e_q^{-E_a/T} e_q^{-E_b/T} = \int 8\pi^2 p_a p_b dE_a dE_b \times d\cos\theta e_q^{-E_a/T} e_q^{-E_b/T}. \quad (37)$$

$$\langle \sigma_{ab} v_{ab} \rangle = \frac{\sigma \int 8\pi^2 p_a p_b dE_a dE_b d\cos\theta e_q^{-E_a/T} e_q^{-E_b/T} \times \frac{\sqrt{(E_a E_b - p_a p_b \cos\theta)^2 - (m_a m_b)^2}}{E_a E_b - p_a p_b \cos\theta}}{\int 8\pi^2 p_a p_b dE_a dE_b d\cos\theta e_q^{-E_a/T} e_q^{-E_b/T}}. \quad (38)$$

Here the cross-section σ is used as a parameter in the calculations. E_a and E_b are integrated in the limit m_a to ∞ and m_b to ∞ , respectively. The integration limit for $\cos\theta$ is -1 to 1. The other thermodynamical quantities using non-extensive statistics are calculated as [38],

$$n = g \int \frac{d^3p}{(2\pi)^3} \left[1 + (q-1) \frac{E-\mu}{T} \right]^{-\frac{q}{q-1}}, \quad (39)$$

$$\epsilon = g \int \frac{d^3p}{(2\pi)^3} E \left[1 + (q-1) \frac{E-\mu}{T} \right]^{-\frac{q}{q-1}}, \quad (40)$$

$$P = g \int \frac{d^3p}{(2\pi)^3} \frac{p^2}{3E} \left[1 + (q-1) \frac{E-\mu}{T} \right]^{-\frac{q}{q-1}}, \quad (41)$$

where n , ϵ and P are the number density, energy density and pressure of hadrons, respectively.

III. RESULTS AND DISCUSSIONS

In this section, we present our findings and corresponding analysis regarding the electrical and thermal conductivities which are obtained by solving the Boltzmann transport equation with non extensive statistics. The parameter q , which denotes how far from thermal equilibrium the system is, affects the relaxation time. By examining the electrical conductivity (σ_{el}) and the thermal conductivity (κ), we investigate how the system behaves with changing q -values for different temperature (T) and baryon chemical potential (μ_B). For the studies done in this paper, we have chosen a temperature range of $T = 90 - 160$ MeV, as a possible hadronic phase is expected to be created below the critical temperature, $T_c \sim 160$ MeV. We have limited ourself to $q < 1.15$ as it has been shown in Ref.[39] that beyond that value there might not be any phase transition which would render the study irrelevant. It is necessary to include all hadrons up to a certain cutoff. For our analysis, we choose the mass cutoff, $\Lambda = 2.0$ GeV. We have taken a constant cross-section, $\sigma = 200$ mb.

First, we want to see the variation of temperature scaled- σ_{el} and κ (to make them dimensionless) with q for

Using the Tsallis non-extensive statistics for q -equilibrium, the $\langle \sigma_{ab} v_{ab} \rangle$ takes the following form,

different temperature and μ_B and then we shall examine the ratio $\frac{\kappa}{\sigma_{el}}$ to see if it is possible to find analogy of hadronic gas within condensed matter systems. For our analysis, we have varied the temperature in the range from 90 MeV to 160 MeV. We have chosen five different baryon chemical potentials: $\mu_B = 25, 45, 200, 436$ and 630 MeV, which is relevant for RHIC at $\sqrt{s_{NN}} = 200, 130, 19.6$ GeV, RHIC/FAIR at $\sqrt{s_{NN}} = 7.7$ GeV and NICA at $\sqrt{s_{NN}} = 3$ GeV, respectively [40–43].

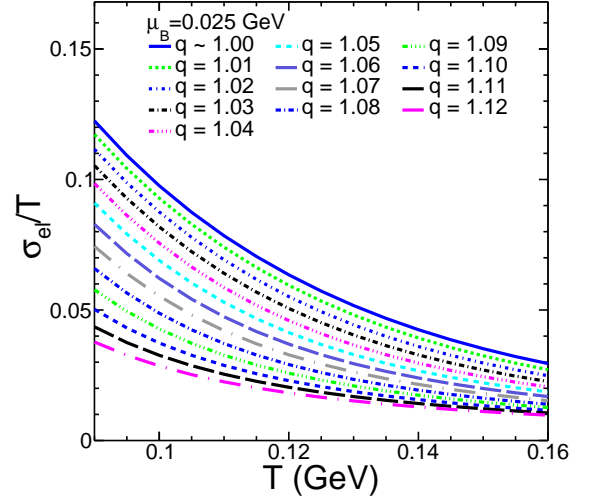


FIG. 1: (Color online) σ_{el}/T vs T for different q -values at $\mu_B = 0.025$ GeV.

In Fig.1 and Fig.2, the temperature scaled- σ_{el} is shown as a function of temperature for different q -values for $\mu_B = 25$ MeV and 436 MeV. We can clearly see that σ_{el} decreases with both temperature and the Tsallis parameter. $q = 1.0001$ roughly corresponds to equilibrium Boltzmann distribution case and higher values of q signifies moving farther away from equilibrium. At $q = 1.0001$, our result shows similar behaviour as observed in Ref.[12] and the values are also in the same ballpark. We observe that σ_{el} decreases more rapidly at lower temperature and

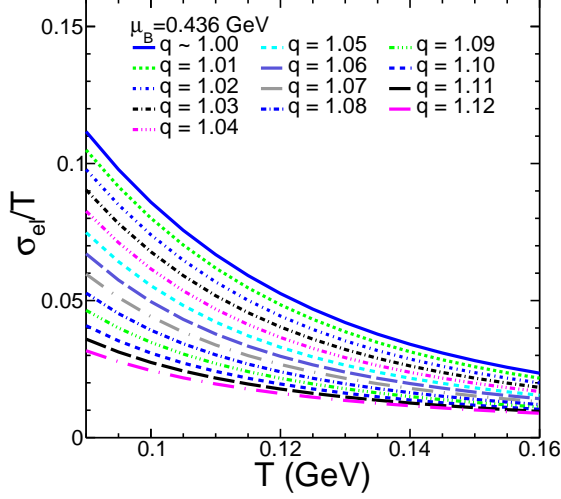


FIG. 2: (Color online) σ_{el}/T vs T for different q -values at $\mu_B = 0.436$ GeV

at higher temperature, the fall is more gradual. Also, we see that the sharp decrease is more prominent at lower q values. This can be understood by examining carefully the expression of σ_{el} in Eq.[15]. Apart from the factor of $\frac{1}{T}$, there are two quantities in the expression which depends on T , μ_B and q : the relaxation time τ and the distribution function f_0 . Of these two quantities, τ decreases sharply with temperature for lower temperature and falls gradually at higher temperature. On the other hand, f_0 increases with temperature but its increase is not sharp enough to combat the fall of τ . So σ_{el} roughly mimics the behaviour of τ . With q also, the same pattern follows. This behaviour of σ_{el} can also be intuitively understood. At higher value of temperature or q , the system experiences more collision between hadrons which effectively reduces the flow of charged particles and hence σ_{el} decreases.

We observe an apparently strange behaviour of σ_{el} with μ_B . From the two figures, it is clear that σ_{el} barely changes with μ_B whereas we would expect it to decrease noticeably since τ decreases significantly. However this can also be understood by examining Eq.[15] and the expression for $\langle\sigma_{ab}v_{ab}\rangle$ in Eq.[38]. The dependence of $\langle\sigma_{ab}v_{ab}\rangle$ on μ_B is very weak, resulting in the relaxation time τ to depend on μ_B in a similar fashion, which is almost exactly countered by the opposite behaviour of f_0 with μ_B . Even more significantly, the contributions to σ_{el} comes only from electrically charged hadrons which in our case is dominated by charged mesons, which does not depend explicitly on μ_B .

Figure 3 shows the variation of σ_{el} both with T and μ_B simultaneously for the equilibrium scenario. Here, we have included results for all different μ_B that has been considered. It is obvious that σ_{el} remains more or less

unchanged for different μ_B except for $\mu_B = 630$ MeV for which σ_{el} changes noticeably at lower temperature. At higher temperature, the change in σ_{el} is negligible as it approaches extremely small value for all μ_B .

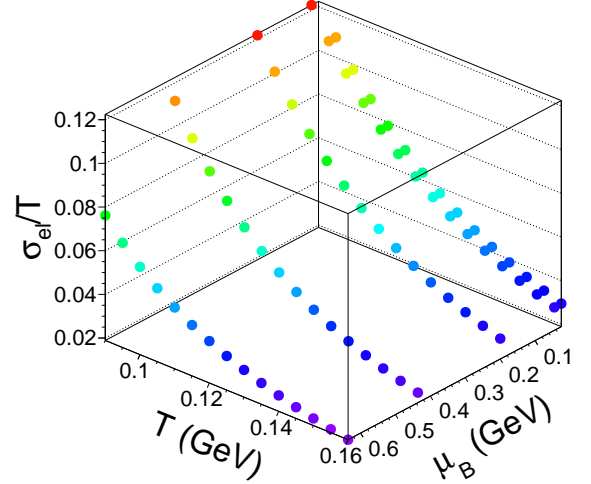


FIG. 3: (Color online) σ_{el}/T as a function of T and μ_B for different center of mass energies at $q \sim 1$

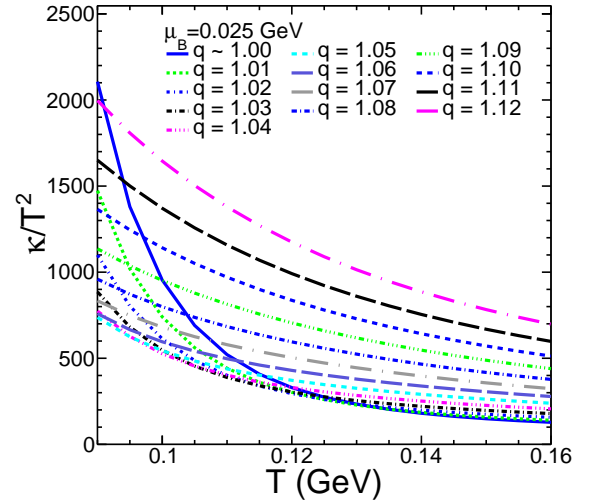


FIG. 4: (Color online) κ/T^2 vs T plot for different q -values at $\mu_B = 0.025$ GeV.

In Fig.4 and Fig.5, thermal conductivity κ is shown as a function of temperature for different q values for $\mu_B = 25$ MeV and 436 MeV. Like the electrical conductivity, κ also decreases with T for all values of q . Also, similar to σ_{el} , the fall is sharper at lower temperature and more gradual at higher temperature roughly mimicking

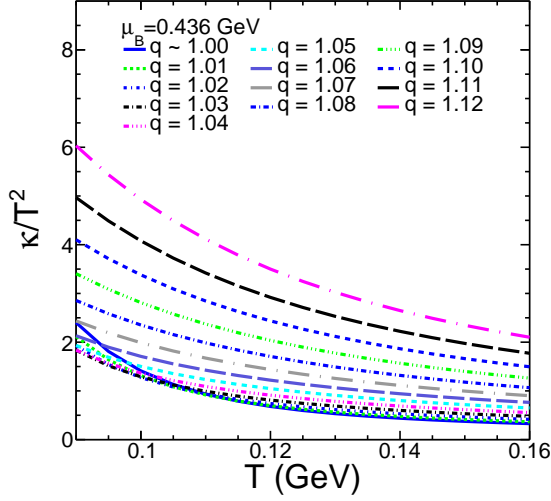


FIG. 5: (Color online) κ/T^2 vs T plot for different q -values at $\mu_B = 0.436$ GeV.

the behaviour of τ . But unlike σ_{el} , κ shows significant variation with μ_B . This is expected as the non-zero contributions to κ comes only from baryons which is sensitive to change in chemical potential. In fact, the fall of κ with μ_B is more dramatic compared to the fall with T . The decrease with μ_B is also largely shaped by the decrease of τ with μ_B as well as the fact that κ gets non-zero contribution from baryons only and μ_B essentially decides how much of the system participates in heat conduction. So contrary to σ_{el} , μ_B is the dominant parameter affecting κ .

However, the variation of κ with q shows more complicated behaviour. At large values of temperature, κ shows clear increase with q . But at lower temperature, smaller values of q tend to yield a larger value of κ . This behaviour has been previously observed for velocity of sound (c_s^2) [39] where c_s^2 was higher for larger q at higher temperature and lower temperature showed opposite behaviour with clear shifting of the peak towards lower temperature for higher values of q .

Figure [6] shows how κ changes with both T and μ_B for equilibrium case. As discussed, we can see that while κ decreases with both T and μ_B , the change with μ_B is much sharper.

Since we have calculated both κ and σ_{el} , it would be interesting to examine the validity of Wiedemann-Franz law which states that for a material that is a good conductor of both heat and electricity, the ratio $\frac{\kappa}{\sigma_{el}}$ is proportional to temperature and the proportionality constant is called Lorenz number. In other words, $\frac{\kappa}{\sigma_{el}T}$ should remain a constant. It has been observed that metals, which is a good conductor of both electricity and heat, follow this law to a reasonably good extent. In present context, we should remember that hadron gas is very

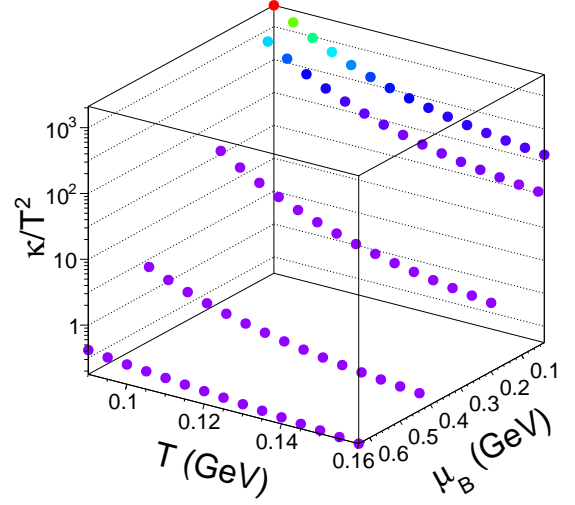


FIG. 6: (Color online) κ/T^2 vs T as a function of T and μ_B for different center-of-mass energies at $q \sim 1$

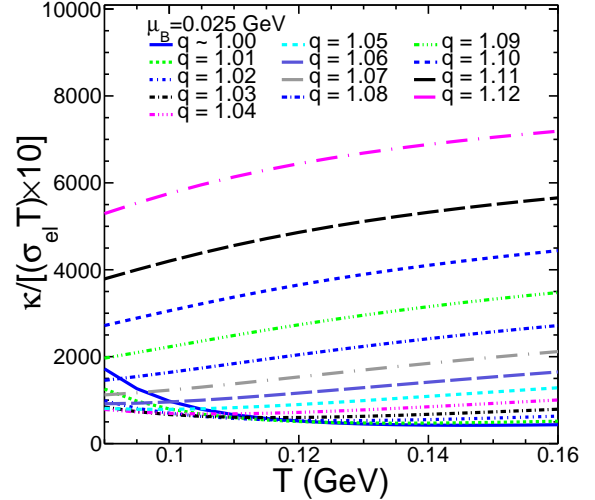


FIG. 7: (Color online) κ/σ_{el} vs T for different q -values at $\mu_B = 0.025$ GeV.

different from metals with very low electrical conduction. In Fig.[7] and Fig.[8], we have shown the behaviour of the Lorenz number with temperature for different q -values. We observed wide variation of Lorenz number with temperature. The Lorenz number decreases with temperature for equilibrium case while increasing significantly when the system is far from equilibrium. In addition, as we shall discuss in the subsequent paragraphs, beyond a certain temperature the Lorenz number tend to increase for any values of the non-extensive parameter, q . We shall also see that this reversal in trend hap-

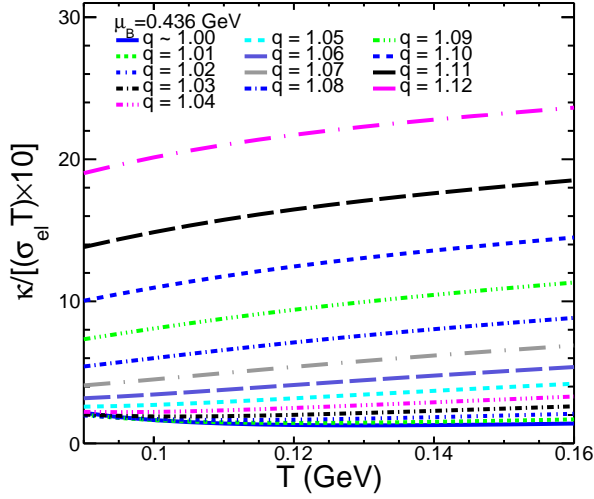


FIG. 8: (Color online) $\kappa/(\sigma_{el}T)$ vs T for different q -values at $\mu_B = 0.436$ GeV.

pens at progressively lower temperatures as we increase the baryochemical potential. However, this violation of Wiedemann-Franz law should not come as a surprise as there are significant differences between a metal and hadron gas. In metals, at low temperature, both electrical and thermal conduction are accomplished by the same particles, i.e., the charged particles whereas in a hadronic gas, they are done by different particles. The electrical conduction is done by any charged hadrons whereas thermal conductivity requires a conserved charge which is baryon number in our case. So, μ_B affects κ significantly while having negligible effects on σ_{el} . This ensures significant decrease in Lorenz number with changing μ_B . Violation of Wiedemann-Franz law has been shown recently in the context of 2-flavor quark matter in Nambu-Jona Lasinio model [44], for hot QGP medium [45] and in quasiparticle model in presence of strong magnetic field [46].

As we have shown for σ_{el} and κ , we show the variation of L with both T and μ_B for equilibrium scenario in Fig.[9]. The Lorenz number decreases with both T and μ_B throughout the phase diagram except for $\mu_B = 630$ MeV where it increases with T . As we can see from Fig.[6], the change in κ with T is very slight for $\mu_B = 630$ MeV and σ_{el} changes faster thus resulting in an increasing trend for L . At this point, it may be interesting to extend the range of the temperature of the study to approximately $2T_c$ to see the behavior of the Lorenz number. In Fig. 10, the $\kappa/(\sigma_{el}T)$, the Lorenz number is shown as a function of the temperature of a hot hadron gas at equilibrium for various values of the baryochemical potentials. It is interesting to observe a minima around T_c , for higher collision energies (low μ_B), which slowly vanishes for a baryon rich matter expected to be formed at NICA energies for which the Lorenz number increases monotonically throughout the range of temperature dis-

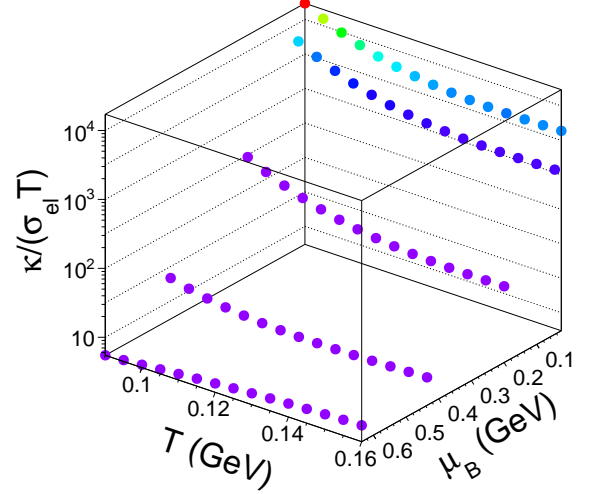


FIG. 9: (Color online) $\kappa/(\sigma_{el}T)$ as a function of T and μ_B for different center of mass energies at $q \sim 1$

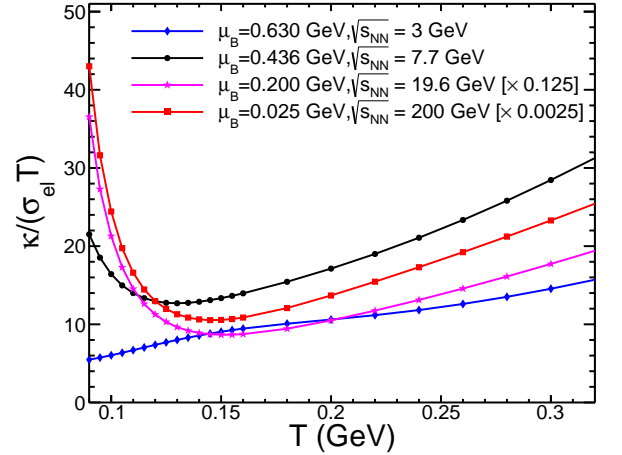


FIG. 10: (Color online) $\kappa/(\sigma_{el}T)$, the Lorenz number for an equilibrated hot hadron gas as a function of T .

cussed here. This behavior is quite interesting and needs further investigation.

In Fig.[11], we have shown the variation of the Lorenz number with the Tsallis non-extensive parameter q . The temperature corresponding to each μ_B in the plot indicates the chemical freezeout temperatures at the mentioned centre-of-mass energies for the relevant experiment. We see that L increases slowly with q for lower values of q and then increases rapidly for any μ_B . This happens as a result of much sharper increase in κ with q compared to σ_{el} . It is worth emphasizing again that we are considering only the freezeout temperature. Had we considered a much lower temperature, we would observe

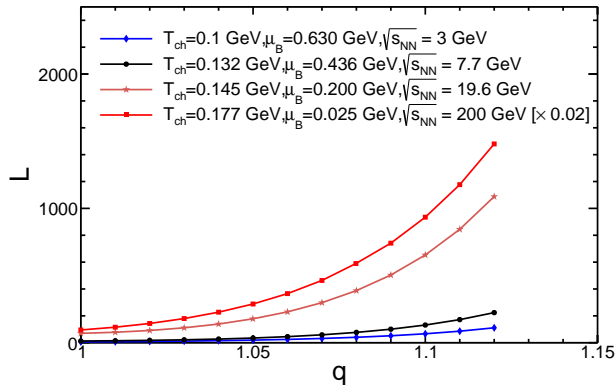


FIG. 11: (Color online) Lorenz number as a function of the non-extensive parameter, q .

exactly opposite behaviour of L with q as κ tends to decrease with increasing q at lower temperature whereas the qualitative behaviour of σ_{el} with q remains the same for any temperature. At very high μ_B , the Lorenz number is very small at small q as κ falls dramatically with μ_B whereas σ_{el} remains relatively unchanged for reasons mentioned above.

IV. SUMMARY

This work is the first attempt to investigate the non-equilibrium effects on thermal and electrical conductivities in the context of a hadron gas. The Tsallis-Boltzmann statistics has been used to include effects of non-equilibrium and solved that Boltzmann transport equation in relaxation time approximation for σ_{el} and κ . We also checked whether the Wiedemann-Franz law holds for hadron gas. This analysis has been carried out at five different baryon chemical potentials, μ_B which are relevant for RHIC, FAIR and NICA experiments. We can summarize our finding as follows.

a) The electrical conductivity σ_{el} decreases as the system moves away from equilibrium, i.e., for higher q -values. This change is significant particularly at lower temperature. The qualitative behaviour of σ_{el} as a function of T and μ_B remains the same for both equilibrium and non-equilibrium scenario and it decreases with both T and μ_B even though the change with μ_B very small.

b) The qualitative behaviour of κ also remains same for equilibrium and non-equilibrium scenario. However, as the system moves away from equilibrium, the change in heat conduction is more complex. At lower temperature, κ is greater for equilibrium case similar to σ_{el} . At higher temperature, particularly near the freezeout temperature, κ increases significantly as the system moves farther and farther from equilibrium.

c) Wiedemann-Franz law is not obeyed in a hadron gas system. The Lorenz number, i.e., the ratio $\frac{\kappa}{\sigma_{el}T}$ decreases with temperature for equilibrium case and increases with temperature significantly as the system moves far from equilibrium. Also, for any given T and μ_B , the Lorenz number increases as the system moves away from equilibrium showing the dominance of heat conduction over electrical conductivity.

d) For an equilibrated hadron gas, the Lorenz number shows an interesting variation with temperature (when taken up to around $2T_c$), when studied for different baryochemical potentials. For higher collision energies, we observe a minima in Lorenz number around T_c , whereas for lower collision energy (relevant for NICA), we don't see such a behavior, rather it shows a monotonic increase with temperature.

This work by no mean presents a complete picture of hadron gas with non equilibrium effects. We have considered only the baryons to be eligible for heat conduction whereas it has been shown that pion number also remains almost constant in the hadronic phase and thus making it eligible for heat conduction. So, for a more complete picture of the phase after chemical freezeout, one should include the effects of pion also. Also, it would be interesting to see the non-equilibrium effects when quarks are present in the system. Some of these works are in progress and will be reported later.

Acknowledgements

The authors acknowledge the financial supports from ALICE Project No. SR/MF/PS-01/2014-IITI(G) of Department of Science & Technology, Government of India. RR and ST acknowledge the financial support by DST-INSPIRE program of Government of India. BC and ST acknowledge fruitful discussions with Dr. Guru Prakash Kadam and Prof. Hiranmaya Mishra. SKT would like to acknowledge the financial support from TEQIP-III- a joint venture of MHRD and the World Bank.

-
- [1] P. Kovtun, D. T. Son and A. O. Starinets, Phys. Rev. Lett. **94**, 111601 (2005).
 - [2] L. P. Csernai, J. I. Kapusta and L. D. McLerran, Phys. Rev. Lett. **97**, 152303 (2006).
 - [3] M. Gyulassy and L. McLerran, Nucl. Phys. A **750**, 30

- (2005).
- [4] D. E. Kharzeev, L. D. McLerran and H. J. Warringa, Nucl. Phys. A **803**, 227 (2008).
- [5] K. Tuchin, Adv. High Energy Phys. **2013**, 490495 (2013).
- [6] K. Fukushima, D. E. Kharzeev and H. J. Warringa, Phys.

- Rev. D **78**, 074033 (2008).
- [7] M. Greif, I. Bouras, C. Greiner and Z. Xu, Phys. Rev. D **90**, 094014 (2014).
 - [8] S. I. Finazzo and J. Noronha, Phys. Rev. D **89**, 106008 (2014).
 - [9] W. Cassing, O. Linnyk, T. Steinert and V. Ozvenchuk, Phys. Rev. Lett. **110**, 182301 (2013).
 - [10] S. x. Qin, Phys. Lett. B **742**, 358 (2015).
 - [11] S. Mitra and S. Sarkar, Phys. Rev. D **89**, 054013 (2014).
 - [12] G. P. Kadam, H. Mishra and L. Thakur, Phys. Rev. D **98**, 114001 (2018).
 - [13] B. I. Abelev *et al.* [STAR Collaboration], Phys. Rev. C **75**, 064901 (2007).
 - [14] A. Adare *et al.* [PHENIX Collaboration], Phys. Rev. C **83**, 064903 (2011).
 - [15] K. Aamodt *et al.* [ALICE Collaboration], Eur. Phys. J. C **71**, 1655 (2011).
 - [16] B. Abelev *et al.* [ALICE Collaboration], Phys. Lett. B **717**, 162 (2012).
 - [17] B. Abelev *et al.* [ALICE Collaboration], Phys. Lett. B **712**, 309 (2012).
 - [18] G. Wilk and Z. Wlodarczyk, Phys. Rev. Lett. **84**, 2770 (2000).
 - [19] C. Tsallis, J. Statist. Phys. **52**, 479 (1988).
 - [20] C. Tsallis, Braz. J. Phys. **29**, 1 (1999).
 - [21] D. Thakur, S. Tripathy, P. Garg, R. Sahoo and J. Cleymans, Adv. High Energy Phys. **2016**, 4149352 (2016) and references therein.
 - [22] P. Sett and P. Shukla, Int. J. Mod. Phys. E **24**, 1550046 (2015).
 - [23] T. Bhattacharyya, J. Cleymans, A. Khuntia, P. Pareek and R. Sahoo, Eur. Phys. J. A **52**, 30 (2016).
 - [24] H. Zheng and L. Zhu, Adv. High Energy Phys. **2015**, 180491 (2015).
 - [25] Z. Tang, Y. Xu, L. Ruan, G. van Buren, F. Wang and Z. Xu, Phys. Rev. C **79**, 051901 (2009).
 - [26] B. De, Eur. Phys. J. A **50**, 138 (2014).
 - [27] S. Tripathy, S. K. Tiwari, M. Younus and R. Sahoo, Eur. Phys. J. A **54**, 38 (2018).
 - [28] S. Tripathy, T. Bhattacharyya, P. Garg, P. Kumar, R. Sahoo and J. Cleymans, Eur. Phys. J. A **52**, 289 (2016).
 - [29] S. Tripathy, A. Khuntia, S. K. Tiwari and R. Sahoo, Eur. Phys. J. A **53**, 99 (2017).
 - [30] S. K. Tiwari, S. Tripathy, R. Sahoo and N. Kakati, Eur. Phys. J. C **78**, 938 (2018).
 - [31] G. P. Kadam and H. Mishra, Phys. Rev. C **92**, 035203 (2015).
 - [32] A. Hosoya and K. Kajantie, Nucl. Phys. B **250**, 666 (1985).
 - [33] J. R. Bezerra, R. Silva and J. A. S. Lima, Physica A **322**, 256 (2003).
 - [34] S. Gavin, Nucl. Phys. A **435**, 826 (1985).
 - [35] O. Moroz, Ukr. J. Phys. **58**, 1127 (2013).
 - [36] M. Cannoni, Phys. Rev. D **89**, 103533 (2014).
 - [37] P. Gondolo and G. Gelmini, Nucl. Phys. B **360**, 145 (1991).
 - [38] J. Cleymans and D. Worku, Eur. Phys. J. A **48**, 160 (2012).
 - [39] A. Khuntia, P. Sahoo, P. Garg, R. Sahoo and J. Cleymans, Eur. Phys. J. A **52**, 292 (2016).
 - [40] N. A. Tawfik, L. I. Abou-Salem, A. G. Shalaby, M. Hanafy, A. Sorin, O. Rogachevsky and W. Scheinast, Eur. Phys. J. A **52**, 324 (2016).
 - [41] P. Braun-Munzinger, D. Magestro, K. Redlich and J. Stachel, Phys. Lett. B **518**, 41 (2001).
 - [42] J. Cleymans, H. Oeschler, K. Redlich and S. Wheaton, Phys. Rev. C **73**, 034905 (2006).
 - [43] A. Khuntia, S. K. Tiwari, P. Sharma, R. Sahoo and T. K. Nayak, arXiv:1809.03780 [hep-ph].
 - [44] A. Harutyunyan, D. H. Rischke and A. Sedrakian, Phys. Rev. D **95**, 114021 (2017).
 - [45] S. Mitra and V. Chandra, Phys. Rev. D **96**, 094003 (2017).
 - [46] S. Rath and B. K. Patra, arXiv:1901.03855 [hep-ph].